Journal of Molecular Graphics and Modelling 74 (2017) 273–287

Contents lists available at ScienceDirect

Journal of Molecular Graphics and Modelling

journal homepage: www.elsevier.com/locate/JMGM

Topical Perspectives

Conformational and energy evaluations of novel peptides binding to dengue virus envelope protein

Asfarina Amir-Hassan[a,b], Vannajan Sanghiran Lee[a,c], Aida Baharuddin[a,d], Shatrah Othman[a,d], Yongtao Xu[e,g], Meilan Huang[e], Rohana Yusof[a,d], Noorsaadah Abd. Rahman[a,c], Rozana Othman[a,b,f,*]

[a] Drug Design & Development Research Group, University of Malaya, 50603 Kuala Lumpur, Malaysia
[b] Department of Pharmacy, Faculty of Medicine, University of Malaya, 50603 Kuala Lumpur, Malaysia
[c] Department of Chemistry, Faculty of Science, University of Malaya, 50603 Kuala Lumpur, Malaysia
[d] Department of Molecular Medicine, Faculty of Medicine, University of Malaya, 50603 Kuala Lumpur, Malaysia
[e] School of Chemistry and Chemical Engineering, Queen's University Belfast, Northern Ireland, United Kingdom
[f] Centre for Natural Product Research and Drug Discovery, University of Malaya, 50603 Kuala Lumpur, Malaysia
[g] School of Biomedical Engineering, Xinxiang Medical University, Xinxiang, Henan 453003, China

ARTICLE INFO

Article history:
Received 10 January 2017
Received in revised form 15 March 2017
Accepted 16 March 2017
Available online 7 April 2017

Keywords:
Peptide
Molecular dynamics simulation
Envelope protein
Docking
Free energy of binding
Dengue

ABSTRACT

Effective novel peptide inhibitors which targeted the domain III of the dengue envelope (E) protein by blocking dengue virus (DENV) entry into target cells, were identified. The binding affinities of these peptides towards E-protein were evaluated by using a combination of docking and explicit solvent molecular dynamics (MD) simulation methods. The interactions of these complexes were further investigated by using the Molecular Mechanics-Poisson Boltzmann Surface Area (MMPBSA) and Molecular Mechanics Generalized Born Surface Area (MMGBSA) methods. Free energy calculations of the peptides interacting with the E-protein demonstrated that van der Waals (vdW) and electrostatic interactions were the main driving forces stabilizing the complexes. Interestingly, calculated binding free energies showed good agreement with the experimental dissociation constant (K_d) values. Our results also demonstrated that specific residues might play a crucial role in the effective binding interactions. Thus, this study has demonstrated that a combination of docking and molecular dynamics simulations can accelerate the identification process of peptides as potential inhibitors of dengue virus entry into host cells.

1. Introduction

Dengue virus (DENV) infections have become a serious public health problem that cause fatal diseases and affect approximately 100 million people annually. Currently, there is no effective therapeutic treatment available to treat the diseases. Dengue virus is transmitted through infected mosquito bites and can cause dengue fever, an illness characterized by fever with rashes, severe back pain and plasma leakage. The clinical manifestations of dengue virus infections range in severity from a simple febrile illness to hemorrhagic fever and a potentially fatal hemorrhagic shock syndrome [1]. Researchers are still searching for the mechanism on how the virus binds to target cells. Basically, dengue virus has a relatively simple structure with envelope (E) protein as the major structural protein exposed on the surface [2]. Therefore, targeting the entry of enveloped viruses into host cells is a very attractive strategy for therapeutic intervention since the inhibitor site of action is likely to be extracellular and relatively accessible, thus could limit cell toxicity. The E-glycoprotein that consists of 495 amino acids was reported to play an important role in the DENV attachment to the host cell receptors and entry into the target cells. Therefore, it is an important target protein for DENV drug development [3,4].

The penetration of an enveloped virus into its target cell is the first stage of the viral replication cycle, and each stage in the cycle can be a potential target for an inhibitor [5]. Since DENV E-protein is a target for antiviral therapy, a variety of compounds have been investigated to inhibit this process. Inhibition of virus attachment is a valuable antiviral strategy because it forms the first barrier to block DENV infection [6]. Basically, domain III E-protein forms an immunoglobin-like module and the presence of this structure, which acts as an adhesive, confirms that E-protein is responsible

* Corresponding author at: Department of Pharmacy, Faculty of Medicine, University of Malaya, 50603 Kuala Lumpur, Malaysia.
E-mail address: rozanaothman@um.edu.my (R. Othman).

http://dx.doi.org/10.1016/j.jmgm.2017.03.010
1093-3263/

for cell attachment [2]. In another study proposed by Alhoot et al. [7], it was found that peptides could inhibit DENV entry by blocking its biological attachment to the host cell and causing structural rearrangements of the viral E-protein. Inhibiting the entry of DENV into host cells to avoid infection is an attractive approach to develop potent and specific antivirals. The putative antiviral molecules targeting entry would not need to enter the cell, thereby avoiding strict structural and chemical constraints in the search and design of these molecules. Blocking the virus before entry could also reduce the hyperactivation of the immune system produced [8]. In a study by Wang et al. [9], a compound was identified as an inhibitor with an average 50% effective concentration of 119 nM against DENV serotype 2 in a human cell line. This compound acted at an early stage during the virus infection by arresting dengue virus in vesicles that colocalized with endocytosed dextran, which led to the inhibition of NS3 expression. This study strongly suggested that this compound interacted with the E-protein and therefore blocked the virus entry process.

In general, ligands such as peptides can be promising leads for drug design and development as they have the capability to block protein–protein interactions. They are basically less toxic, highly flexible, and can adopt a variety of conformations in solution depending on the temperature and solvent conditions. These peptides, however, are biologically active only when they fold into specific highly complex shapes. Theoretically, the process of peptide folding could be simulated *in silico*. In the case of DENV infection, synthetic molecules that have the ability to mimic binding or functional sites of proteins are useful for exploring and modulating protein function, as they can interfere with the protein function. Consequently, peptides that mimic specific regions of E-protein can be good candidates for the inhibition of protein–protein interactions. Thus, these peptides can be excellent candidates as protein binding site mimics [10]. Some of these peptides that bind to E-protein may cause changes in the glycoproteins organization on the viral surface [4]. Previous research [11] had shown that the design of peptides as inhibitors was considered good enough to inhibit the activity of DENV protein.

Recently, multiple inhibitory peptides were designed using computational predictive strategies together with high-resolution structural data of DENV E-protein [12]. Two peptides showed inhibition of viral entry by interfering with virus binding to the host cell surface. Similarly, other peptides derived from the stem of DENV E-protein showed blocking of viral fusion and inhibition of infectivity. The activity of these peptides depends upon their affinity for the conformational intermediate because they bind to the virus before attachment and are carried with virions into endosomes where the acidification initiates the fusion [7].

The ability of a protein to interact with small molecules plays an important role in the protein dynamics, which may enhance or inhibit its biological function. Therefore, it is important to be able to predict which is the site that enables specific biological functions such as inhibition or catalysis. This study reports the modelling of peptide-protein complexes using SwarmDock algorithm, where flexible docking of four novel peptides into DENV E-protein was performed. The SwarmDock docking server has been validated in the CAPRI (Critical Assessment of Prediction of Interactions) blind docking experiments and is the highest performing server currently available [13]. After uploading PDB files of the binding partners, the SwarmDock docking server generates low energy conformations and returns ranked list of clustered docking poses and their corresponding structures.

Additionally, molecular dynamics (MD) simulation was performed in this study to investigate the interactions between protein and peptides along the simulation time. MD simulation allows flexibility to the ligand and protein receptor, thus facilitating the relaxation of the complete system and accounting for induced fit effects. The effect of solvent molecules may be treated explicitly, with the incorporation of water molecules in simulated system, so that water-mediated interactions can be studied. Since most of the biological reactions occur in water, solvent effects become an important aspect in analytical and numerical molecular modelling. MD simulation was also performed to measure the complex stability through free energy of binding calculation. In this case, Molecular Mechanics Poisson-Boltzmann Surface Area (MMPBSA) and Molecular Mechanics Generalized Born Surface Area (MMGBSA) approaches were used to evaluate the binding free energy of peptide-E-protein complexes. In addition, both Poisson Boltzmann (PB) and Generalized Born (GB) explicit solvent models were successfully applied to calculate the energy contribution of each residue toward the binding free energy on a decomposition basis for each of the peptide-E-protein system [14]. MMPBSA/GBSA calculation considers the interactions, including van der Waals, electrostatic and desolvation energies, between all inter- and intramolecular pairs of protein and peptide residues [15]. Analysis of the results obtained may provide interesting information such as electrostatic and van der Waals energies, solvation energy and entropic contributions at the binding interface.

2. Methodology

2.1. Materials

The three-dimensional structure of pre-fusion dengue virus E-protein was retrieved from the Protein Data Bank (http://www.rcsb.org/pdb; PDBid: 1OKE). The pre-fusion structure (dimeric form) of dengue virus type 2 (DEN-2) was used in this study as a model for the computational method to design peptide entry inhibitors [7]. For the protein molecules, all heteroatoms which included the drugs, chlorine atoms, water, glycerol and molecules originating from the crystallization buffers were removed. In this study, the peptides encoded as DS36opt, DS36wt, DN58opt and DN58wt were designed by Xu et al. [12] using a Monte Carlo method. These peptides comprised of short sequences of 20–29 amino acids (Table 1).

The sequence for the wild type peptides, which are ^{351}LITVNPIVTEKDSPVNIEAE^{370} (DS36wt) and ^{374}GDSYIIIGVEPGQLKENWFKKGSSIGQMF^{394} (DN58wt), are located in the DIII region of the E-protein. These peptide sequences were generated by moving a 20-amino-acid sliding window from the N- to the C- terminus of the DENV E-protein in an increment of 10 amino acids. The sliding window of 20 amino acids was chosen for this purpose as it is the approximate length of potential inhibitory peptides [17]. To generate the optimized peptides, DS36opt and DN58opt, the wild type peptides (DS36wt and DN58wt) were then used as templates for amino acids mutations, respectively. For each of the peptides, the position for amino acid mutation was selected randomly and the selected amino acid was replaced by one of the other 19 naturally occurring amino acids. The optimized peptides obtained were minimized using the AMBER ff99SB force field. The peptide stability, which indicated its potential to bind to E-protein, was evaluated using two scoring functions, namely dDFIRE (Dipolar Distance scaled, Finite, Ideal-gas reference state) and RAPDF (all-atom probability discriminatory scoring function) [12].

2.2. In silico *peptide folding*

AMBER 12 program [18,19] was used to model the 3D structures of the peptides. Peptide folding was performed to simulate the possible starting structures of the peptides prior to docking. Wild type peptides with codes DS36wt and DN58wt have 100% identity to

Table 1
Relationship between the binding activity ($K_{d,exp}$) obtained from fluorescence quenching assay [16] and the binding free energy (ΔG_{bind}) calculated using the Swarmdock docking algorithm.

Peptide code	Peptide sequence	ΔG_{bind} (kcal/mol)	$K_{d,exp}$ (μM)
DS36opt	RHWEQFYFRRRERKFWLFFW	−32.18	9.31 ± 0.15
DS36wt	LITVNPIVTEKDSPVNIEAE	−22.35	N/A
DN58opt	TWWCFYFCRRHHPFWFFYRHN	−34.18	9.44 ± 0.28
DN58wt	GDSYIIIGVEPGQLKENWFKKGSSIGQMF	−22.22	10.79 ± 0.17

N/A = Not Available.

parts of DENV EIII-protein amino acid sequence, while the newly optimized peptides with codes DS36opt and DN58opt are totally different compared to the wild type amino acid sequence [12].

All the peptide folding simulations started with extended conformations of the peptides to demonstrate that these peptides could be folded from an arbitrary starting structure [20]. Topology and parameter files of the unfolded peptides (wild type and optimized peptides) were generated via the xLEAP program of the AMBER 12 simulation package [21]. The peptide folding simulation was performed using an all-atom classical simulation with AMBER ff99SB force field. The best 3D model was selected according to the lowest energy generated by ptraj program, considering that the lowest energy model indicates peptide stability, and thus, peptide structure quality.

Energy minimization and MD simulations were subsequently performed using PMEMD.CUDA module in AMBER 12 [18,19] on NVIDIA GPU Quadro 600, which sped up the simulation time with a factor of 22.6–31.7, an improvement over the fastest CPU implementation to obtain the trajectory files from each simulation. A short minimization (total of 1000 steps) of the starting structure was performed, which comprised 500 steps of steepest descent followed by 500 steps of conjugate gradient. This process did not cause the peptide to completely fold since minimization only drive the starting structure to a local minimum. It should reduce steric clashes of the structure, fix hydrogen atom positions so that the system had stabilised prior to MD simulation. Since the system was small, non-bond energy cutoff was not employed in the calculation of the full Generalised Born solvation energy.

For the MD simulation, the system was heated up over time step of 50 picoseconds in a total of 7 stages. Heating in stages reduced the chances that the system would blow up by allowing it to equilibrate at each temperature change. Normally, MD simulation would be run at 300 K. In this study, the system was heated up to 325 K to avoid being kinetically trapped in local minima leading to a faster folding pathway [20]. A time step of 2 femtoseconds was used to integrate the equations of motion. The SHAKE algorithm was used to fix the bond distances consisting of hydrogen and heavy atoms, and the Berendsen thermostat was used for temperature control. Finally, peptide folding was simulated for 100 ns at a constant temperature of 325 K and pressure (1 atm) by the Berendsen weak-coupling algorithm.

2.3. Docking of peptides to DENV E-protein

For each peptide, the folded structure with the lowest energy along the 100 ns simulation was chosen as the starting structure for docking to DENV E-protein (PDB ID = 1OKE). Docking was performed using the SwarmDock server (www.bmm.cancerresearchuk.org/~SwarmDock/), which performs flexible protein–protein docking using the SwarmDock algorithm where the peptide and side chains of E-protein were kept flexible throughout the docking runs. This docking program was used to predict and assess the interactions between DENV E-protein and peptides. The server work started with the pre-processing of input structures where the structures were checked for structural correctness, modelling of missing and non-standard residues, and minimization of structures using the CHARMM molecular mechanics package. This was then followed by docking of the peptides using a hybrid particle swarm optimisation where a set of approximately 120 starting positions were generated so that they evenly spaced around the receptor protein. The whole docking process was repeated four times at each starting position and the best structure found during the optimisation was kept for the final post-processing stage. The job was then submitted to the server as a full blind docking case. After docking had completed, all the poses underwent minimization using CHARMM force field. The minimized structures were subsequently re-ranked using a centroid potential. Finally, these structures were clustered and results for this submission were then returned in PDB formatted structures, allowing for visualization of the clustered solutions [13].

2.4. Molecular dynamics simulations of peptide-E-protein complexes

Each docked peptide-E-protein complex structure with the best pose and lowest binding energy was selected for MD studies using AMBER 12 program. Each complex was solvated with a truncated octahedral box of TIP3P water with the box boundaries of at least 12 Å from the complex, and was neutralized with Na^+ and Cl^- ions. The fully solvated system was then minimized in two stages. The first stage involved minimization of the peptide with 500 steps of steepest descent followed by 500 steps of conjugate gradient with a force constant of 500 kcal/mol. The second stage of minimization was run on the whole peptide-E-protein complex with 1000 steps of steepest descent followed by 1500 steps of conjugate gradient minimization without restraints. Minimization was followed by simulation with parameters comprised of the time step of 2 femtoseconds, Langevin thermostat set to 310 K, and electrostatic interactions were treated using the particle mesh Ewald method. The SHAKE algorithm [22] was applied to constrain all hydrogen-heavy atom bonds. Then, the complex was heated from 0 to 310 K for 200 picoseconds and submitted to molecular dynamics in NPT (constant number of particles, pressure and temperature) ensemble for 30 ns. During this phase, structural coordinates of the system were taken at 0.1 picosecond intervals to build a trajectory of the system dynamics. Time-dependent properties were calculated from the production trajectory. The convergence of the energies and root mean square deviation (RMSD) were checked to indicate the system stability.

2.5. Analyses of results

The structures of the peptide-E-protein complexes were verified using Ramachandran plot [23] and Verify3D programs [24]. A Ramachandran plot was generated to check for the stereochemical quality of each peptide-E-protein complex at selected time simulation. Additionally, Verify3D software was used to determine the compatibility of the 3D atomic models with their own 1D amino acid. Incorrect segments of a model usually have profile window plots approaching or falling below a score of zero (with

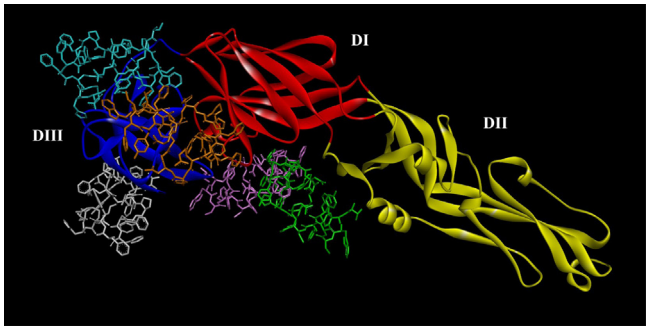

Fig. 1. Five best conformations for the peptide DN58opt, docked to DENV E-protein generated from Swarmdock program. DI, DII, DIII are illustrated in red, yellow and blue colours, respectively. The peptides (illustrated as sticks; different colours indicate different binding positions) are associated to different domains of the E-protein. Peptides in turquoise and white bound to DIII were further investigated.

Verify3D, scores below 0.1 indicate a serious problem in the model). The Ramachandran plot was generated from the online RAMPAGE server at http://mordred.bioc.cam.ac.uk/~rapper/rampage.php [23]. Meanwhile, the Verify3D program [25] is available in the online server version at the Structural Analysis and Verification Server of UCLA (University of California, Los Angeles; http://services.mbi.ucla.edu/SAVES/). Results obtained were analysed and visualized using Visual Molecular Dynamics (VMD) program [26]. Interactions between the peptides and E-protein in the docked complexes were analysed using Discovery Studio Visualizer [27] and Ligplot [28] softwares which identified the hydrogen bonding and hydrophobic interactions between the E-protein and the peptides.

2.5.1. Calculation of free energy of binding

The free energy of binding (ΔG_{bind}) of each complex was calculated based on Molecular Mechanics Poisson Generalized Born Surface Area (MMPBSA) and Molecular Mechanics Generalized Born Surface Area (MMGBSA) procedures [29] in AMBER 12 program. In this study, the binding free energy of each system was calculated in two simulation time range, which are 7–10 ns and 25–30 ns, within which the complexes appeared to gain stable configurations. A total of 500 snapshots were collected for estimation of the free energy of binding (ΔG_{bind}). The free energy of binding of a protein-ligand complex is calculated following the relationship shown below [30]:

$$\Delta \mathbf{G}_{bind} = \mathbf{G}_{complex} - G_{protein} - G_{ligand} \quad (1)$$

$$= \mathbf{E}_{MM} + \mathbf{G}_{GB/PB} + \mathbf{G}_{nonpolar} - T\Delta S$$

where $G_{complex}$, $G_{protein}$ and G_{ligand} are the free energies of the complex, protein (monomer) and ligand (monomer), respectively; E_{MM} is the change of the molecular mechanics potential energy upon peptide binding that includes van der Waals (E_{vdW}) and electrostatic (E_{ele}) energies; $G_{GB/PB}$ and $G_{non\text{-}polar}$ are the polar and non-polar components of the desolvation free energy, respectively; and $-T\Delta S$ is the change of conformational entropy upon peptide binding which was not considered in this study because of the high computational cost required and the tendency for a large error margin that will lead to significant uncertainty in the results [31,15,14].

2.5.2. Analysis of the decomposition of free energy

Free energy decomposition for each peptide-E-protein complex was examined to obtain information on the important residues involved in the complex binding. The energy decomposition was carried out by using the mm_pbsa.pl implemented in the AMBER 12 package to calculate the per-residue decomposition. Per-residue decomposition calculates the energy contribution of single residues

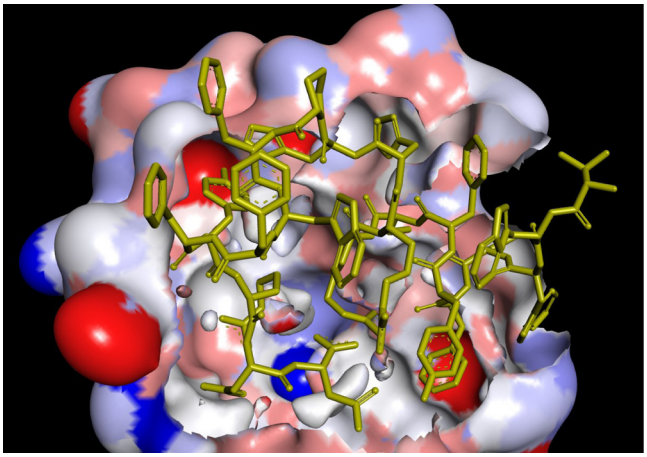

Fig. 2. Transparent Connolly surface representation of peptide DN58opt at the binding site.

by integrating the interactions of each residue over all residues in the system. The per-residue decomposition involves the separation of the energy contribution of each residue from the association of receptor with the ligand into three terms: van der Waals contribution (ΔE_{vdW}), electrostatic contribution (ΔE_{ele}) and solvation contribution ($\Delta G_{gb} + \Delta G_{surf}$) [32]. In this study, the decomposition of free energy of peptide-E-protein complex was calculated based on the MMPBSA and MMGBSA protocols. By using the MMPBSA and MMGBSA programs in AMBER 12, the energy contribution of each residue was divided into three parts: van der Waals energy (ΔG_{vdW}), intermolecular electrostatic energy (ΔG_{ele}), and solvation energy (ΔG_{sol}) due to solvent effect, which was a sum of the polar solvation energy (ΔG_{GB}) and the non polar solvation energy (ΔG_{SA}):

$$\Delta \mathbf{G}_{residue\_pair} = \Delta \mathbf{G}_{vdW} + \Delta G_{ele} + \Delta G_{solvation}$$

$$= \Delta \mathbf{G}_{vdw} + \Delta G_{ele} + \Delta G_{GB} + \Delta G_{SA} \quad (2)$$

where ΔG_{vdW} and ΔG_{ele} are nonbonded van der Waals and electrostatic interactions between two residues, respectively.

In this study, the decomposition of free energy of each system was calculated from the 7–10 ns and 25–30 ns window of the trajectories from where 500 snapshots were extracted. The interaction energy profiles were generated by decomposing the total binding free energies into residue–residue interaction.

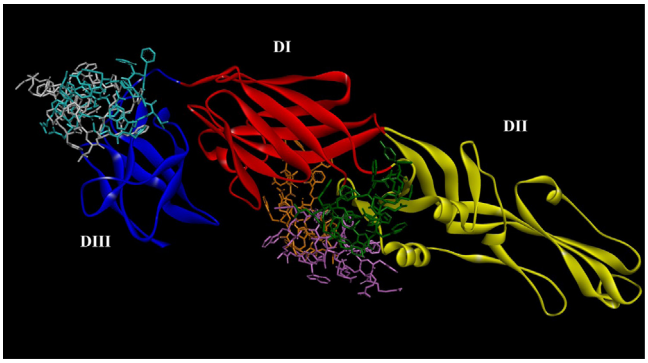

Fig. 3. Five best conformations for the peptide DS36opt, docked to DENV E-protein generated from Swarmdock program. DI, DII, DIII are illustrated in red, yellow and blue colours, respectively. The peptides (illustrated as sticks; different colours indicate different binding positions) are associated to different domains of the E-protein. Peptides in turquoise and white bound to DIII were further investigated. (For interpretation of the references to colour in this figure legend, the reader is referred to the web version of this article.)

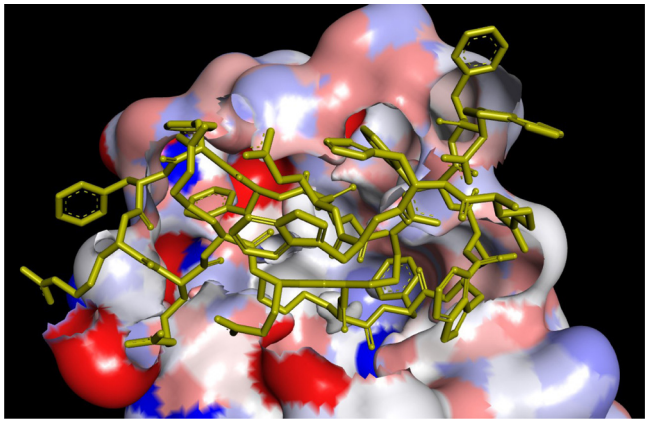

Fig. 4. Transparent Connolly surface representation of peptide DS36opt at the binding site.

3. Results and discussion

3.1. Docking studies for modelling peptide-E-protein complexes

The binding energy (Table 1) of each peptide-E-protein complex was calculated using the Swarmdock algorithm, where flexible peptide was docked into the protein binding site with flexible side chains. In this study, docking analysis was employed to get the best orientation and binding affinity of a peptide to its protein receptor. The negative binding energies for all these peptides indicated favourable binding in all the complexes, which concluded that the peptides were able to locate the binding site within the protein receptor. In this case, the system underwent induced fit because the protein continuously changed its conformation and shape in response to peptide binding. The same phenomenon could also be observed in small-molecule binding, even when the protein was relatively rigid [33]. Basically, peptides used in these study gave better binding energy compared to peptides studied by Hrobowski et al. [17], where it was reported that the binding energies ranged from −19.2 to −21.5 kcal/mol. Furthermore, the trend of the binding energy of each complex was in agreement with the results reported for the tryptophan fluorescence quenching assay performed by Baharuddin et al. [16]. Good correlations between the docking scores and the dissociation constant ($K_{d,exp}$) values could be observed, as shown in Table 1. Since the peptides with codes DS36opt and DN58opt gave the lowest binding energy values, they were then used in the following MD simulation experiments. Figs. 1 and 3 illustrate the best five conformations for DN58opt and DS36opt docked to DENV E-protein, respectively. Three possible binding sites were located: a) between domains I and II (DI and DII), b) between domains II and III (DII and DIII), and c) domain III (DIII). The best docking pose with the lowest binding energy was located at DIII, which was also the potential site for antibody binding as well as other small molecules [34,35] (Figs. 2 and 4).

3.2. Refinement of docked peptide-E-protein complexes using MD simulation

MD simulation was performed on the best docked complex structure to investigate the role of receptor flexibility on the binding of these peptides in aqueous solution. In addition, MD simulation was performed to assess the stability of each peptide with DIII of E-protein throughout the simulation time. The best docking pose was further refined using explicit solvent MD simulations. To validate the dynamic stability of the complexes, total potential energy and root mean square deviation (RMSD) of the backbone atoms along 30 ns MD trajectories were monitored. Figs. 5 and 6 illustrate the total potential energy and RMSD profiles, respectively, involving peptides DS36opt and DN58opt. The potential energy remained constant for the remaining of the simulation, implying that the temperature thermostat was working properly, and the relaxation, as well as equilibrium, was completed [36].

Table 2
Validation reports for the complexes after MD simulation runs using PROCHECK and Verify3D programs.

Ramachandran Plot	DS36opt		DN58opt	
	10 ns	20 ns	10 ns	30 ns
Most favoured region (%)	93.4	94.1	93.7	92.9
Additional allowed region (%)	6.1	5.4	5.8	6.6
Disallowed region (%)	0.5	0.5	0.5	0.5
Verify 3D (%)	86.47	86.71	91.81	93.98

The trajectory obtained from the MD simulation was used to study conformational changes and structural properties over the simulation time. For this purpose, the RMSD values were calculated for the peptide-E-protein complexes (Fig. 6). In order to get these values, ptraj tool was used and as usual, the backbone atoms C, C_α and N were considered. The RMSD values were observed to oscillate steadily up to 20 ns simulation for both of the peptides under study (DS36opt and DN58opt). The constant RMSD value also indicated that the complexes had successfully equilibrated. The complex containing peptide DN58opt continued to exhibit a constant value of RMSD up to 30 ns, suggesting that the complex was stable throughout the 30 ns simulation with no large conformational changes, and that the peptide remained in the protein binding pocket. On the other hand, the RMSD value of the complex containing DS36opt was initially found to be stable in the range 3–7 Å at 0–19 ns but increased up to 30 Å after 19.5 ns (Fig. 6). This complex continued to fluctuate wildly at around 25 Å within 20–23 ns due to large structural changes of the peptide, and this unsteady pattern demonstrated that the peptide was quite unstable. It can be postulated that peptide DS36opt could have denatured and instantaneously formed a complex structure which was not

Table 3
Binding free energies predicted on the basis of MMPBSA and MMGBSA at different time simulation. (All data are given in kcal/mol).

Method	Contribution	DS36opt	DN58opt	
		7–10 ns	7–10 ns	25–30 ns
MM	ELE	−137.25	−273.4	−251.74
	VDW	−14.85	−74.71	−68.82
	GAS	−152.1	−348.1	−320.56
MMPBSA	PBSUR	−3.07	−13.25	−12.41
	PBCAL	141.09	291.86	263.89
	PBSOL	138.02	278.61	251.48
	PBELE	3.84	18.47	12.15
	PBTOT	**−14.08**	**−69.49**	**−69.08**
MMGBSA	GBSUR	−1.56	−8.11	−7.39
	GBCAL	146.32	298.91	270.11
	GBSOL	144.77	290.81	262.71
	GBELE	9.07	25.52	18.37
	GBTOT	**−7.33**	**−57.29**	**−57.84**

The individual energy contributions: ELE = electrostatic energy as calculated by the molecular mechanics (MM) force field; vdW = van der Waals contribution from MM; GAS = total gas phase energy ELE + vdW + INT; INT = internal energy arising from bond, angle and dihedral terms in the MM force field (this term always amounts to zero in the single trajectory approach); PBELE/GBELE = sum of the electrostatic solvation free energy and MM electrostatic energy; PBSUR/GBSUR = non-polar contribution to the solvation free energy calculated by an empirical model; PBCAL/GBCAL = the electrostatic contribution to the solvation free energy calculated by PB or GB respectively; PBSOL/GBSOL = sum of non-polar and polar contributions to solvation free energy (PBSUR + PBCAL); PBTOT = final estimated binding free energy calculated by MMPBSA method; GBTOT = final estimated binding free energy calculated by MMGBSA method (all energies are in kcal/mol).

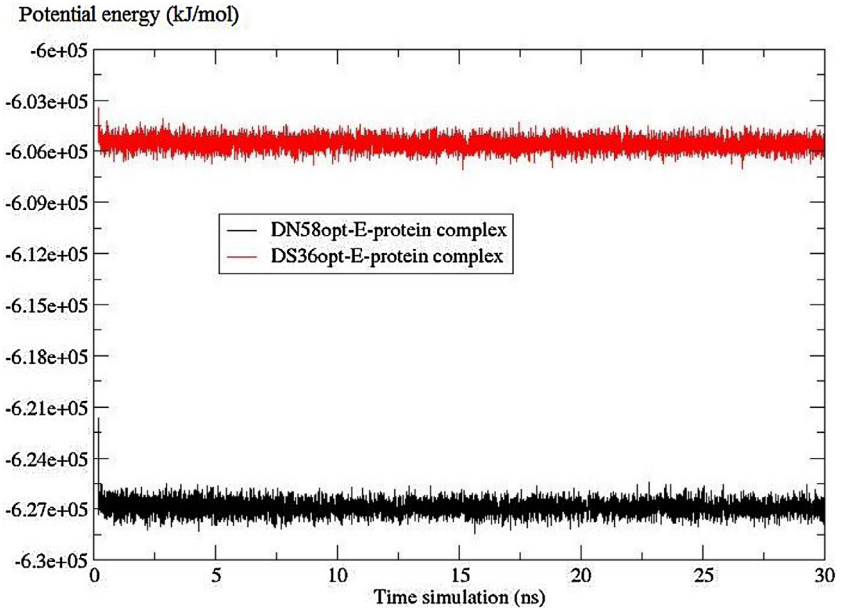

Fig. 5. Potential energy of peptide-E-protein complexes for 30 ns simulation. The heating process is not shown.

energetically stable under the standard AMBER force field. This would also indicate that the peptide was not bound to the receptor anymore. According to Martinez [37], high RMSDs indicate that the whole structure fluctuates or might reflect large displacements of a small structural subset within an overall rigid structure. In addition, high RMSD might come from differences in a flexible region of the ligand or from a nearly correct pose of a symmetric molecule [38]. In their study, Day et al. [39] observed an increment in C_α RMSD of chymotrypsin inhibitor 2 (CI2) from ~4 Å to ~8 Å going into denatured state. Consequently, it is suggested that the complex containing DN58opt possessed greater stability than the complex containing DS36opt. Thus, subsequent analysis up to 30 ns only focused on the DN58opt-E-protein complex.

3.3. Validation of 3D model structures of peptide-E-protein complexes

In this section, the quality of the docked peptide-E-protein complexes, generated by MD trajectories were evaluated. Ramachandran plot and Verify3D programs were used to examine the geometry and stereochemistry of the DS36opt-E-protein and DN58opt-E-protein complexes (Figs. 7 and 8 respectively). The final refined structures of the complexes showed that more than 90% of the residues were located in the most favoured region with few residues (0.5%) in the disallowed region. Results revealed that, at 10 ns, 93.4% and 93.7% of the residues for the complex containing DS36opt and DN58opt, respectively, are located in the most favoured region (Table 2). As the simulation is extended to 20 ns,

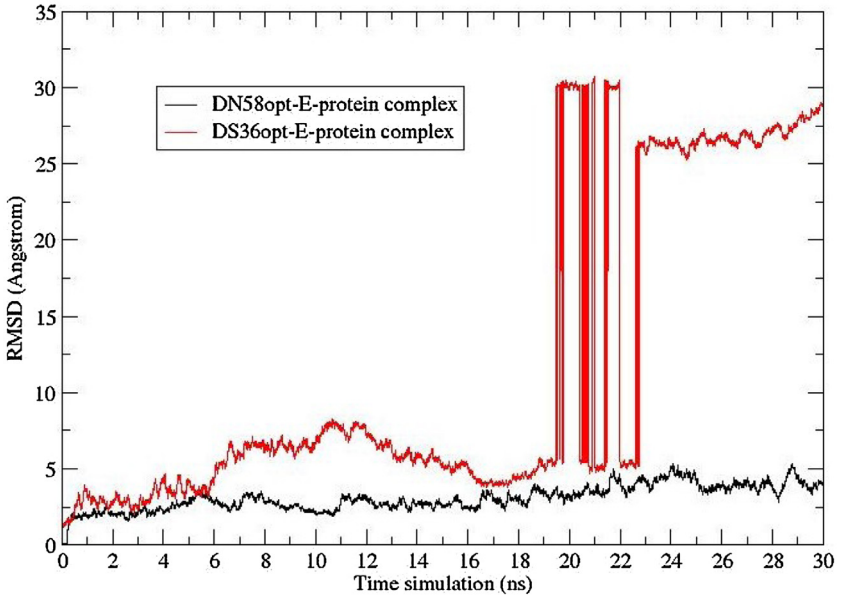

Fig. 6. Root mean square deviation (RMSD) of the backbone atoms of peptide-E-protein complexes within a 30 ns simulation.

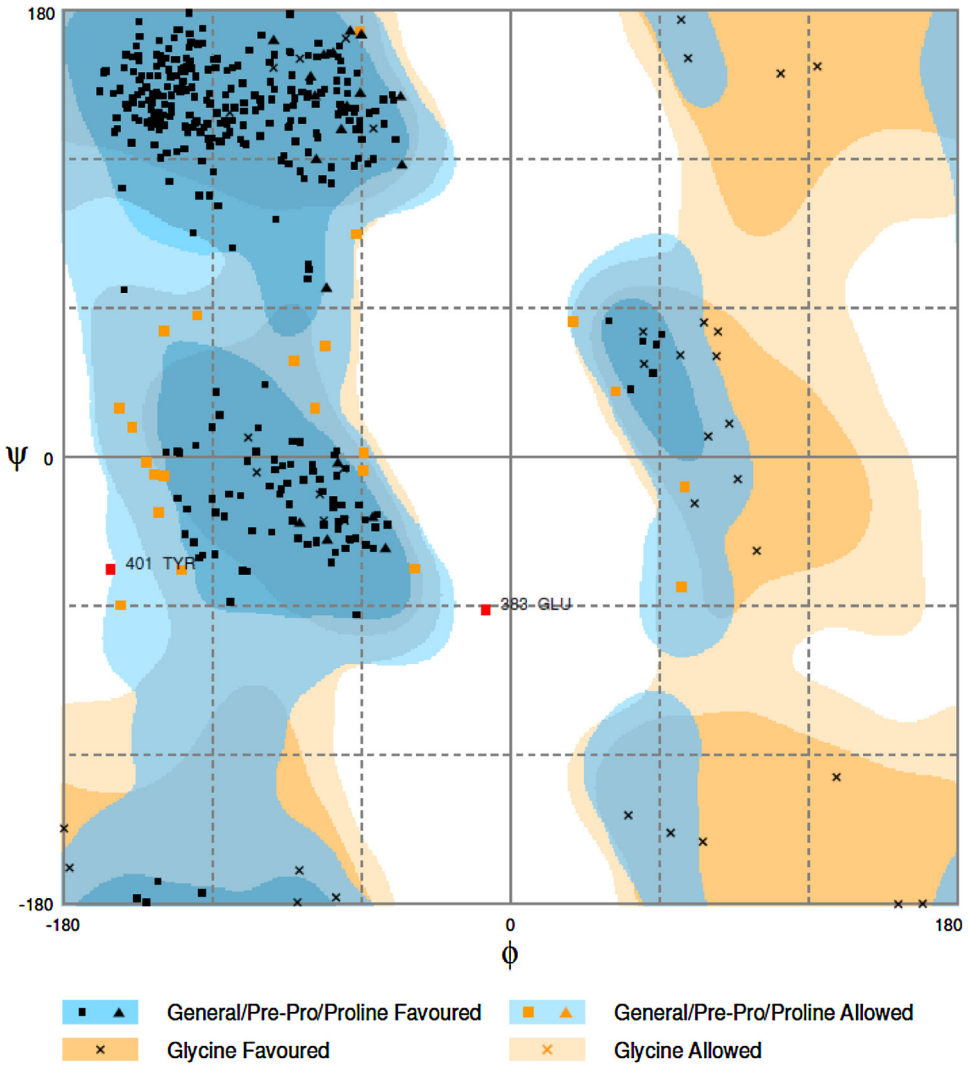

Fig. 7. Ramachandran plot for DS36opt-E-protein complex at 20 ns MD simulation.

residues located in the most favoured region for DS36opt-E-protein complex increase to 94.1% and for DN58opt-E-protein complex at 30 ns, slightly decrease to 92.9%. These results suggested that the peptide-E-protein complex structures were acceptable and possessed sufficient stereochemical qualities. Meanwhile, the 0.5% residue in the disallowed region is not a major concern as these amino acids were not located in any of the peptide binding region. Analysis with Verify3D revealed that the complexes contained adequate 3D atomic models that were compatible with their 1D amino acid sequences, with more than 85% of the residues with an averaged 3D to 1D score of more than 0.2 (Table 2). The results obtained highlighted that all the complex structures were of reasonable quality.

3.4. Binding free energy of peptide-E-protein complexes

Docking results (Table 1) revealed the binding affinities of the peptides to protein to be in the order of DN58opt > DS36opt > DS36wt > DN58wt. As a result, complexes for the two peptides with the highest binding affinities were selected for MD studies to understand the binding interactions involved. Table 3 shows the MMPBSA and MMGBSA binding energy values computed from explicit solvent MD trajectories. Interestingly, the binding free energy obtained from the Swarmdock algorithm (Table 1), and from the MMPBSA and MMGBSA methods (Table 3) after MD simulations showed similar pattern to the experimental K_d values [16]. In this work, MMPBSA and MMGBSA methods of calculation for the binding free energy (ΔG_{bind}) of the peptide-E-protein complexes were employed over the course of 30 ns trajectories.

In order to investigate the peptide binding capability to E-protein in aqueous solution, the results derived from MMPBSA and MMGBSA calculations were compared. Both methods had been successfully applied to various protein-ligand [40] or protein-protein/peptide complexes [41,14] where the performances depended on the system under study [42]. It could be

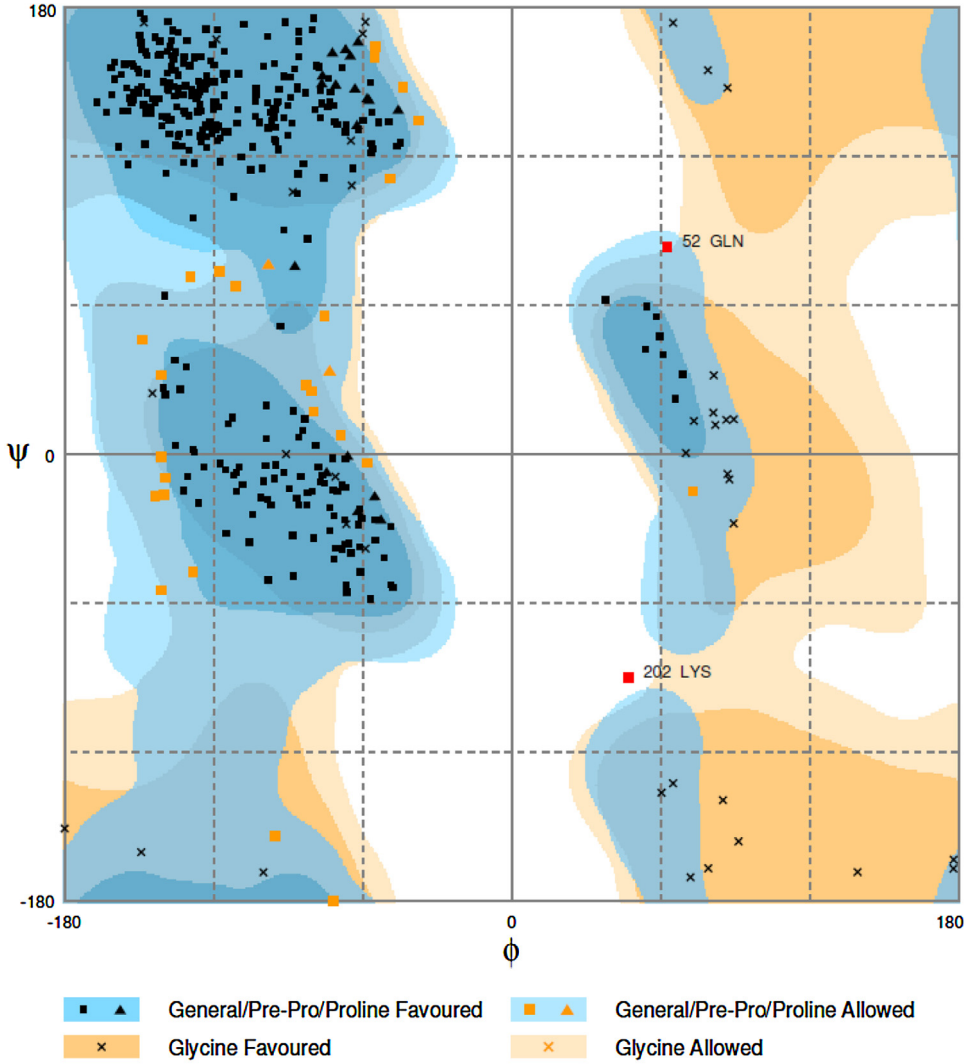

Fig. 8. Ramachandran plot for DN58opt-E-protein complex at 30 ns MD simulation.

observed that MMPBSA gave lower PBTOT value than MMGBSA in both peptides studied (Table 3). Even though the MMGBSA approach gave a slightly higher binding energy, the results obtained in this study still suggested that the complexes were in their favourable bound states. The individual energy contributing to the calculation of the binding free energy, based on MMPBSA and MMGBSA methods, are listed in Table 3. In general, a more negative value of the binding energy, indicates a more favourable binding. The complex containing DN58opt has the most favourable binding energy, followed by DS36opt, where the binding energies during the range of 7–10 ns simulation were −69.49/−57.29 kcal/mol and −14.08/−7.33 kcal/mol (MMPBSA/MMGBSA), respectively. In addition, DN58opt-E-protein complex also showed the same trend for simulation at 25–30 ns where the energy values were −69.08/−57.84 kcal/mol (MMPBSA/MMGBSA). Both Generalised Born and Poison Boltzmann models gave quantitatively very similar trend and this indicated the favourable binding of the peptides to E-protein.

The difference in values obtained for the binding energies could be due to the different force fields used in both of the methods, in addition to the different algorithms. SwarmDock incorporated the CHARMM force field for the docking process, while AMBER ff99SB was used for MD simulation (MMPBSA/MMGBSA). In general, both methods gave the same trending results, that is, the complex containing DN58opt exhibited better binding affinity than that containing DS36opt. The selected calculation methods are just tools used to give description on the binding affinity, which could lead us to the peptide that has inhibitory potential. The SwarmDock docking algorithm has been selected as this server is widely used and has shown considerable success in the critical assessment of predicted interactions (CAPRI) experiments [13]. Meanwhile, MMPBSA and MMGBSA methods are used for post-processing of the docked structures in order to improve the docking results.

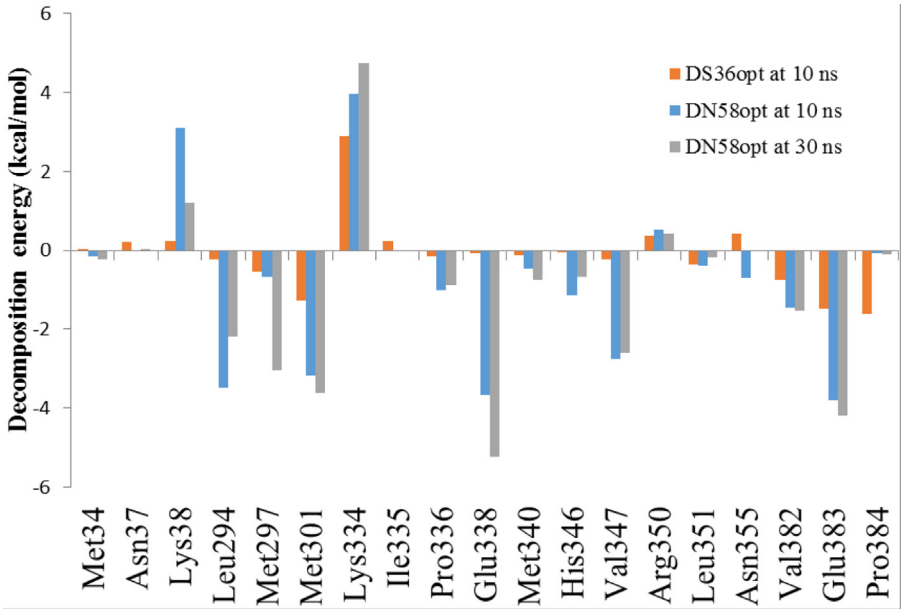

Fig. 9. Histogram showing the calculated per-residue free energy decomposition using MMPBSA approach.

Normally, the major contributors to the binding free energy are the van der Waals (vdW) and electrostatic (ELE) energies, as calculated in this study using the molecular mechanics (MM) force field. However, the polar solvation free energies (PBCAL) were shown to be unfavourable to the binding, as indicated by the positive values, which were 141.09 kcal/mol and 291.86 kcal/mol (at 7–10 ns) for DS36opt and DN58opt, respectively, and 263.89 kcal/mol for DN58opt at 25–30 ns simulation time. On the other hand, results showed that energy contribution from PBSUR for DS36opt and DN58opt were −3.07 kcal/mol and −13.25 kcal/mol (7–10 ns), respectively, and −12.41 kcal/mol for DN58opt at of 25–30 ns time range. These negative values indicated that PBSUR was a favourable component, even though the absolute values were relatively small. The PBSUR term is the non-electrostatic contribution of solvation effects and is proportional to the solvent-accessible surface area of the molecule [43]. The gas-phase electrostatic value (ELE) of DN58opt showed highly negative value (−251.74 kcal/mol), indicating that electrostatic interactions were important factor for the binding. In this study, electrostatic interactions are important forces in the primary approach of peptide and receptor to each other. These types of interactions are of long-range type and can be determinative in the final peptide-E-protein complex stability [44].

The role of van der Waals and electrostatic interactions upon peptide binding were computed to study the forces that led to the most stable conformation. The presence of these interactions that contributed to the binding free energy play an important role in distinguishing the bioactivity of the peptides. The total binding free energy (PBTOT) is the sum of ELE, vdW and PBSOL, and these energies contributed favourably to the peptide binding. This is in line with the study by Pardo [45] that showed vdW interaction being the main energy term favouring peptide binding affinity. Generally, larger peptides that have more atoms will have more vdW interactions. In this case, DN58opt showed lower vdW energy values (−74.71 and −68.82 kcal/mol within 7–10 ns and 25–30 ns, respectively) compared to DS36opt (Table 3). DN58opt fitted more snugly within the binding cavity leading to a tighter binding to E-protein (Fig. 2). This favourable fit between the peptide and E-protein could

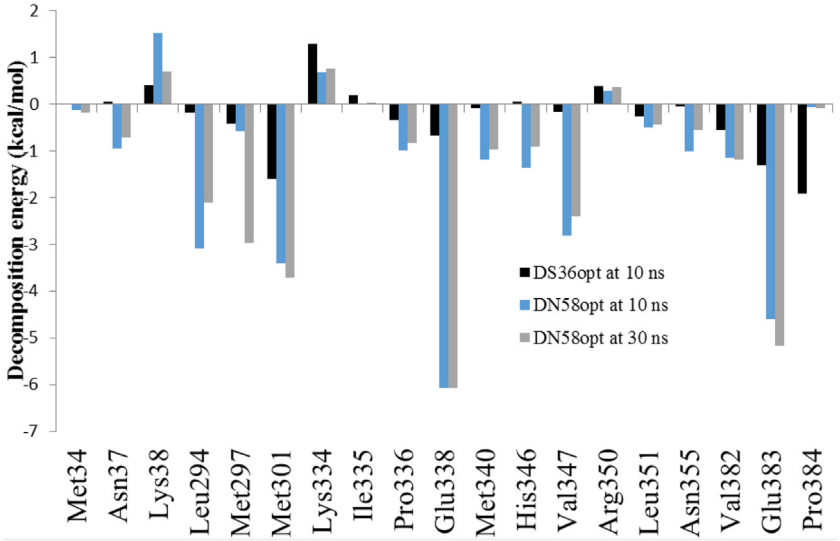

Fig. 10. Histogram showing the calculated per-residue free decomposition energy using MMGBSA approach.

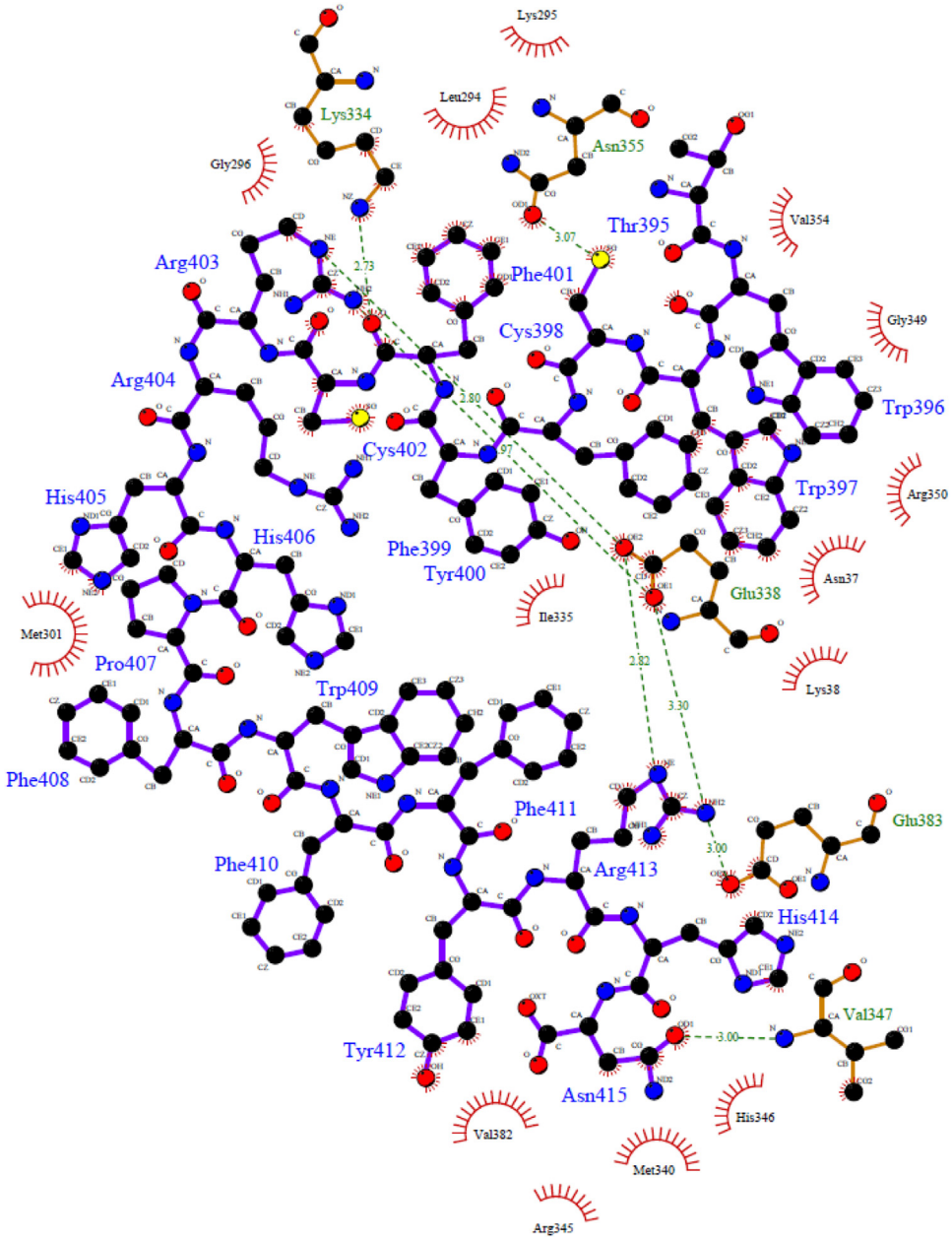

Fig. 11. Schematic diagram (2D) of residues in the binding site which exhibit interactions with peptide DN58opt at 10 ns MD simulation, obtained using the Ligplot program. Keys for the plot are as follows: Peptide DN58opt is shown in stick and ball, H-bonds are shown as dashed green lines and hydrophobic contacts are indicated with spoked red arcs. (For interpretation of the references to colour in this figure legend, the reader is referred to the web version of this article.)

be due to shape complimentary, in addition to the comparatively more vdW interaction. On the other hand, less favourable vdW contributions were found for the shorter peptide, DS36opt, with energy value of −14.85 kcal/mol. The vdW energy difference between these two peptides was quite large (ΔvdW = 59.86 kcal/mol and 53.97 kcal/mol for 7–10 ns and 25–30 ns respectively), which indicated that the vdW interactions are an important factor for binding affinity. Meanwhile, the non polar contributions (PBSUR) and the molecular mechanical internal energies have a less significant contribution to the binding [46].

3.5. Per-residue free energy decomposition (DC) analysis

To identify important residues of the E-protein that interact with the peptide, per-residue free energy decomposition (DC) analysis had been performed. This process has been characterized by means of the evolution of the decomposition of the binding free energy, which provides an energetic profile of the interaction [41]. To accomplish this, enthalpic contribution to the binding free energy was decomposed into its residual components. Based on the contribution of residues to the binding free energy difference, the ones having significance in binding were identified. Figs. 9 and 10 show energy contribution of each residue to the binding free energy using both MMPBSA and MMGBSA approaches. Each amino acid residue was found to exhibit positive or negative influence on the binding to the E-protein. Several residues were identified to give effective contributions to the stabilization energy if their relative energy was found to be larger than 1 kcal/mol [32]. It could be seen that for DN58opt, the residues that could be responsible for binding and complex stabilization were Leu294 (DC energy at 10 ns = −3.48 kcal/mol), Met301 (DC energy at 10 ns = −3.18 kcal/mol),

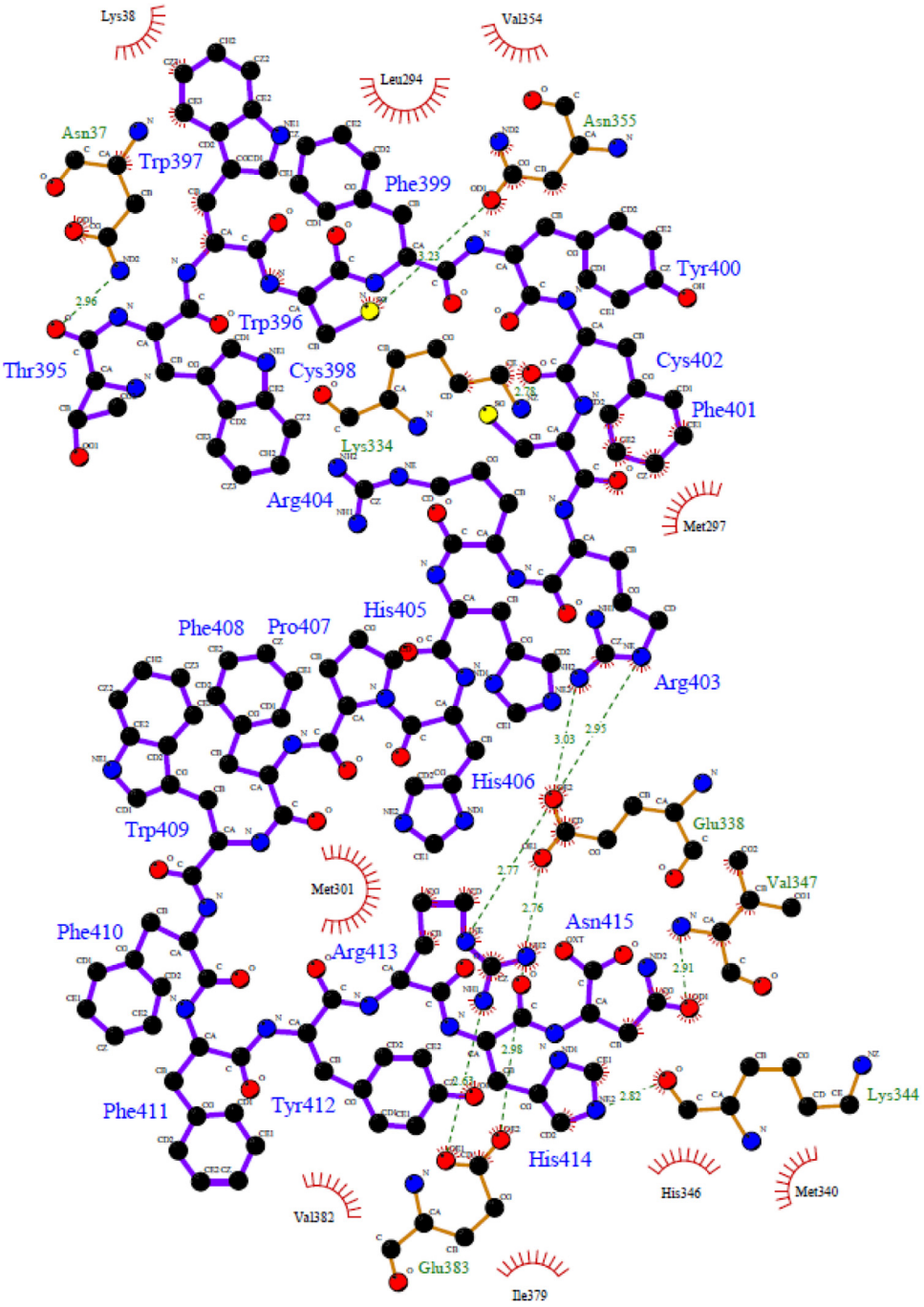

Fig. 12. Schematic diagram (2D) of residues in the binding site which exhibit interactions with peptide DN58opt at 30 ns MD simulation, obtained using the Ligplot program. Keys for the plot are as follows: Peptide DN58opt is shown in stick and ball, H-bonds are shown as dashed green lines and hydrophobic contacts are indicated with spoked red arcs. (For interpretation of the references to colour in this figure legend, the reader is referred to the web version of this article.)

Pro336 (DC energy at 10 ns = −1.01 kcal/mol), Glu338 (DC energy at 10 ns = −3.67 kcal/mol), Met340 (DC energy at 10 ns = −0.47 kcal/mol), His346 (DC energy at 10 ns = −1.15 kcal/mol), Val347 (DC energy at 10 ns = −2.75 kcal/mol), Val382 (DC energy at 10 ns = −1.45 kcal/mol) and Glu383 (DC energy at 10 ns = −3.79 kcal/mol) calculated at MMPBSA level. The combination of polar and hydrophobic residues clearly showed that they might form side chain or side chain-main chain hydrogen bonds with the peptide. It could be noted that Glu338 showed a highly favourable interaction with DN58opt (−3.67 and −5.22 kcal/mol at 10 ns and 30 ns, respectively) indicating that this charged amino acid could make favourable contact in the binding. Residues Glu338, Val347, Asn355, Glu383, and Lys334 also formed H-bond interactions with DN58opt, where it is believe that the presence of hydrogen bonds may stabilize the peptide in its binding site. In contrast, energy contributions from Lys38, Lys334 and Arg350 (3.11, 3.95 and 0.53 kcal/mol, respectively, at 10 ns, and 1.19, 4.75 and 0.41 kcal/mol, respectively, at 30 ns) could play opposite roles in structural stability resulting in weakening of complex stability. This positive energy could be due to the charged residues being energetically able to make favourable contact with water [47].

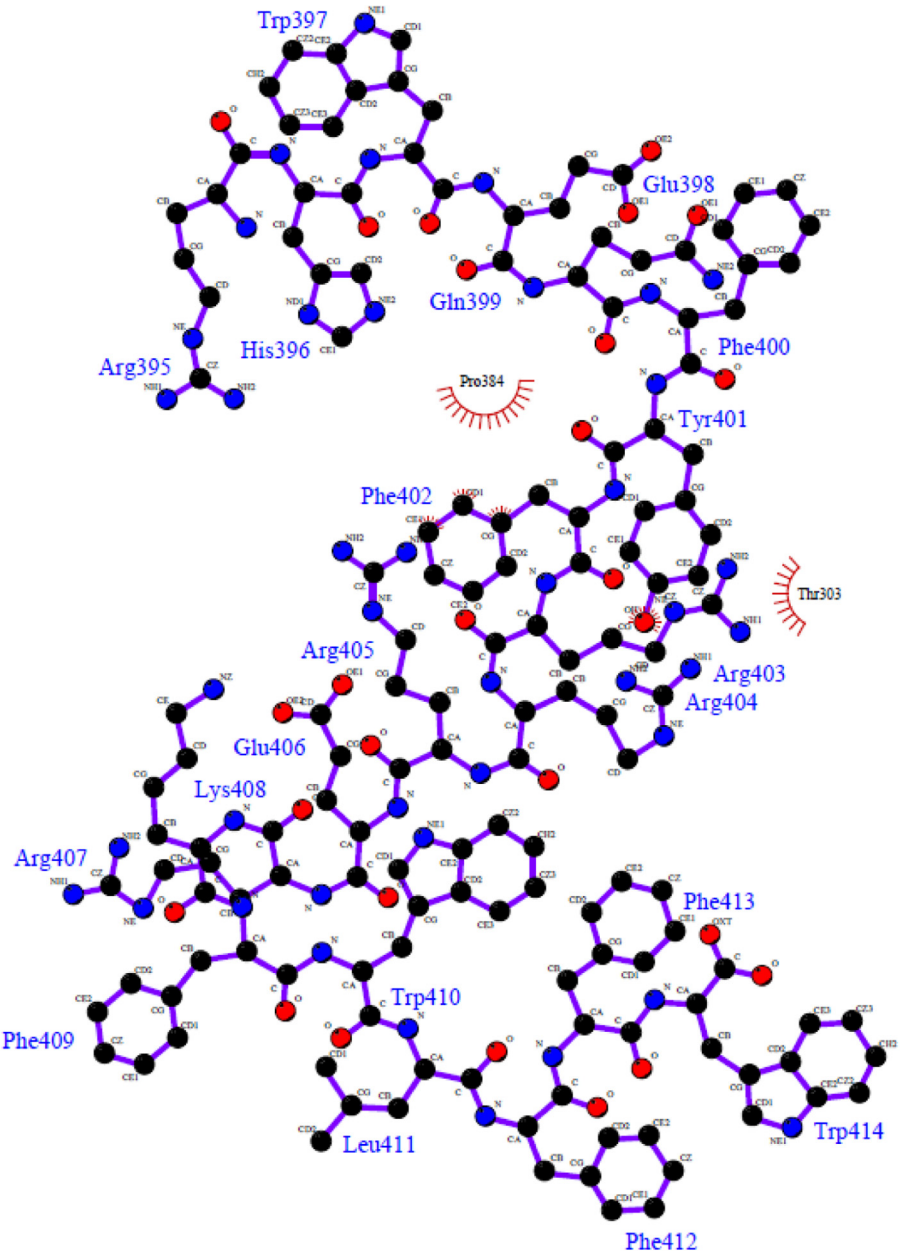

Fig. 13. Schematic diagram (2D) of residues in the binding site which exhibit interactions with peptide DS36opt at 10 ns MD simulation, obtained using the Ligplot program. Keys for the plot are as follows: Peptide DS36opt is shown in stick and ball, H-bonds are shown as dashed green lines and hydrophobic contacts are indicated with spoked red arcs. (For interpretation of the references to colour in this figure legend, the reader is referred to the web version of this article.)

For the peptide DS36opt, residues that contributed most to the interactions were Met297, Met301, Val382, Glu383 and Pro384 (DC energy calculated at MMPBSA level were −0.54, −1.27, −0.76, −1.47 and −1.60 kcal/mol, respectively) while residues Asn37, Lys38, Lys334, Ile335, Arg350 and Asn355 (DC energy calculated at MMPBSA level 0.20, 0.24, 2.90, 0.24, 0.38 and 0.42 kcal/mol, respectively) weakened the stability of the DS36opt-E-protein complex. It was notable that Pro384 was the key residue that had the lowest energy (−1.6 kcal/mol), and this energy contribution could mainly be driven by hydrophobic interaction. Pro384 is a residue that gives rigidity to the protein structure by imposing certain torsion angles on the protein chain, although the overall contribution to the binding free energy by this residue is relatively small.

3.6. Analysis of peptide-E-protein interactions

In order to aid the identification of the possible peptide that can bind to E-protein, it is important to identify the structural features contributing to the interactions. Interactions between the peptide and E-protein were analysed using the LIGPLOT program, which portrayed the hydrogen bonding interaction patterns and hydrophobic contacts between the peptide and active site residues [48]. Hydrogen bond (H-bond) analysis was performed on the peptide-E-protein complexes to determine the possibility of hydrogen bond formation. The criteria for H-bonding interaction used was when the distance between the hydrogen and the heteroatom was within the range of 2.5–3.5 Å, and the bond angle was at 109°–110° [49]. In this study, H-bond analysis and the hydrophobic interactions derived from LIGPLOT indicated the importance of amino acids that contributed to the binding interactions.

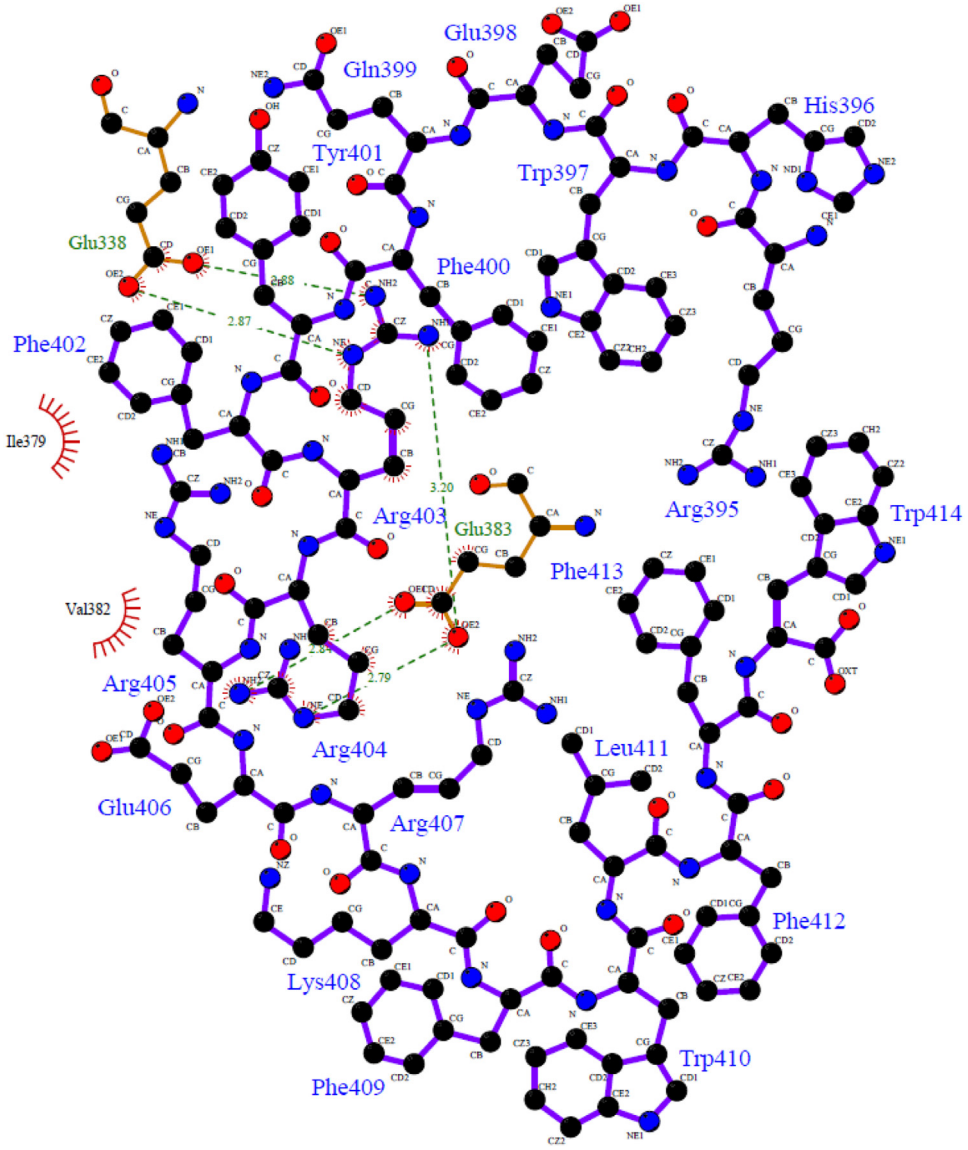

Fig. 14. Schematic diagram (2D) of residues in the binding site which exhibit interactions with peptide DS36opt at 20 ns MD simulation, obtained using the Ligplot program. Keys for the plot are as follows: Peptide DS36opt is shown in stick and ball, H-bonds are shown as dashed green lines and hydrophobic contacts are indicated with spoked red arcs. (For interpretation of the references to colour in this figure legend, the reader is referred to the web version of this article.)

Results obtained from the Tryptophan fluorescence quenching assay [16] and the current docking experiment highlighted that DS36opt and DN58opt are promising peptides to be developed as entry inhibitors against DENV. Figs. 11–14 illustrate the binding interactions of DN58opt and DS36opt at the binding site of E-protein. It could be seen that at 10 ns, DN58opt formed H-bonds with five polar residues namely Lys334, Glu338, Val347, Asn355 and Glu383 (Fig. 11). Interestingly, as the simulation was extended up to 30 ns, DN58opt formed H-bonds with the same polar residues with the addition of one amino acid which is Asn37 (Fig. 12). Complex containing DN58opt (at 10 ns) also formed hydrophobic contact with the following hydrophobic amino acids: Asn37, Lys38, Leu294, Lys295, Gly296, Met301, Ile335, Met340, Arg345, His346, Gly349, Arg350, Val354 and Val382. However, the hydrophobic contacts became less as the simulation was extended to 30 ns and the residues involved with these interactions were reduced to Lys38, Leu294, Met297, Met301, Met340, Val354, His346, Ile379 and Val382. This could explain why the value of PBTOT/GBTOT at 30 ns lower compared to 10 ns simulation (Table 3). Hydrogen bonds and hydrophobic interactions are important indicators of a stable complex [46]. These interactions indicate that neither the typical mode of binding nor the total binding energy are clear predictors in determining how good the peptide could work as inhibitor. Additionally, DN58opt also formed van der Waals and electrostatic interactions with all residues mentioned above (Table 3). Therefore, this underlined the favourable interactions between DN58opt and E-protein as energetically favourable and stable. On the other hand, DS36opt did not demonstrate H-bonding interaction with any of the surrounding residues, but interacted with residues Thr303 and Pro384 via hydrophobic interaction at 10 ns simulation time (Fig. 13). Interestingly, at 20 ns simulation, H-bond interactions were observed with residue Glu338 and Glu383, while hydrophobic interaction was observed to be with residues Ile379 and Val382 (Fig. 14). All these residues highly conserved in protein families since it is crucial in preserving a particular protein 3D fold. This might be the cause of reduction in binding affinity of DS36opt as compared to DN58opt, which is in agreement to the previously reported tryptophan quenching experiment, where the K_d values for DN58opt and DS36opt were 9.44 ± 0.28 μM and 9.31 ± 0.15 μM, respectively [16].

4. Conclusion

In this study, molecular dynamics simulations were performed on selected designed peptides to evaluate their interactions with dengue E-protein in aqua, and to investigate the binding free energy by means of MMPBSA and MMGBSA calculations and energy decomposition analyses. Root mean square deviation (RMSD) was used to ensure the overall structural stability of the peptide-E-protein complexes. Results showed that the calculated binding free energies concurred well with the tryptophan florescence quenching assay previously reported, thus confirming the binding affinities of these novel peptides with Domain III of dengue E-protein. In addition, it was found that the electrostatic and van der Waals interactions contributed mostly during the interactions between the E-protein and the peptides throughout the simulation. Additionally, several amino acids had been identified for their major contributions to the binding efficiency towards E-protein. It can be suggested that these amino acids can later be modified by mutation to improve the binding activity. Consequently, this study provides a combination of computational and experimental methods which can be used to design and generate molecules with desired qualities. The synthetic peptide proposed herein (DN58opt) may serve as a starting point for the development of such a molecule as potential anti-dengue therapeutic.

Author contributions

The manuscript was written through contributions of all authors. All authors have given approval to the final version of the manuscript.

Acknowledgements

This research was supported by MyBrain15 from Malaysia Ministry of Higher Education and grants from the University of Malaya (UMRG RP002/2012C, RP027A-15AFR, and UM-QUB collaboration). We would also like to acknowledge Aurigene Discovery Technologies, India, for the peptides as well as CRYSTAL and Information Technology Centre, University of Malaya, for the computer resources.

References

[1] C.H. Heh, R. Othman, M.J.C. Buckle, Y. Sharifuddin, R. Yusof, N.A. Rahman, Rational discovery of dengue type 2 non-competitive inhibitors, Chem. Biol. Drug Des. 82 (2013) 1–11.
[2] Y. Chen, T. Maguire, R.M. Marks, Demonstration of binding of dengue virus envelope protein to target cells, J. Virol. 70 (12) (1996).
[3] M. Ilyas, Z. Rahman, S. Shamas, M. Alam, M. Israr, K. Masood, Bioinformatics analysis of envelope glycoprotein E epitopes of dengue virus type 3, Afr. J. Biotechnol. 10 (18) (2011) 3528–3533.
[4] S.M. Lok, J.M. Costin, Y.M. Hrobowski, Andrew R. Hoffmann, D.K. Rowe, P. Kukkaro, S.F. Michael, Release of dengue virus genome induced by a peptide inhibitor, PLoS One 7 (11) (2012) 1–8.
[5] E. Teissier, F. Penin, E.I. Pecheur, Targetting cell entry of enveloped viruses as an antiviral strategy, Molecules 16 (1) (2010) 221–250.
[6] M.M.F. Alen, S. Dominique, Dengue virus entry as target for antiviral therapy, J. Trop. Med. (2012) 1–9.
[7] M.A. Alhoot, A.K. Rathinam, S.M. Wang, R. Manikam, S.D. Sekaran, Inhibition of dengue virus entry into target cells using synthetic antiviral peptides, Int. J. Med. Sci. 10 (6) (2013) 719–729.
[8] C.D.L. Guardia, R. Lleonart, Review article: progress in the identification of dengue virus entry/fusion inhibitors, BioMed. Res. Int. 2014 (2014) 13, Article ID 825039 http://dx.doi.org/10.1155/2014/825039.
[9] Q.-Y. Wang, S.J. Patel, E. Vangrevelinghe, H.Y. Xu, R. Rao, D. Jaber, S.G. Vasudevan, A small molecule dengue virus entry inhibitor, Antimicrob. Agents Chemother. 53 (5) (2009) 1823–1831.
[10] J. Meier, K. Kassler, H. Sticht, J. Eichler, Peptides presenting the binding site of human CD4, for the HIV-1 envelope glycoprotein gp120, J. Org. Chem. 8 (2012) 1858–1866.
[11] A.A. Parikesit, Kinanty, U.S. Tambunan, Screening of commercial cyclic peptides as inhibitor envelope protein dengue virus through molecular docking & molecular dynamics, Pak J. Biol. Sci. 16 (24) (2013) 1836–1848.
[12] Y. Xu, N.A. Rahman, R. Othman, P. Hu, M. Hu, Computational identification of self inhibitory peptides from envelope protein, Proteins 80 (9) (2012) 2154–2168.
[13] M. Torchala, I.H. Moal, R.A.G. Chaleil, J. Fernandez-Recio, P.A. Bates, SwarmDock: a server for flexible protein–protein docking, Bioinformatics 29 (6) (2013) 807–809.
[14] P. Tue-nguen, K. Kodchakorn, P. Nimmanpipug, N. Lawan, S. Nangola, C. Tayapiwatana, V.S. Lee, Improved scFv anti-HIV-1 p17 binding affinity guided from the theoritical calculation of pairwise decomposition energies & computational alanine scanning, BioMed Res. Int. 2013 (2013) 1–12.
[15] T. Hou, Z. Xu, W. Zhang, W.A. McLaughlin, D.A. Case, Y. Xu, W. Wang, Characterization of domain-peptide interaction interface a generic structure-based model to decipher the binding specificity of SH3 domains, Mol. Cell. Proteomics 8 (2009) 639–649.
[16] A. Baharuddin, A.A. Hassan, R. Othman, Y. Xu, M. Huang, B.A. Tejo, S. Othman, Dengue envelope domain III-peptide binding analysis via trytophan flourescene quenching assay, Chem. Pharm. Bull. 62 (10) (2014) 947–955.
[17] Y.M. Hrobowski, R.F. Garry, S.F. Michael, Peptide inhibitors of dengue virus and West Nile virus infectivity, Virol. J. 2 (49) (2005) 1–10.
[18] R. Salomon-Ferrer, D.A. Case, R.C. Walker, An overview of the amber biomolecular simulation package, Wiley Interdiscip. Rev.: Comput. Mol. Sci. 3 (2) (2013) 198–210.
[19] R. Salomon-Ferrer, A.W. Gotz, D. Poole, S.L. Grand, R.C. Walker, Routine microsecond molecular dynamics simulations with AMBER on GPUs. 2. Explicit solvent particle Mesh Ewald, J. Chem. Theory Comput. 9 (2013) 3878–3888.
[20] C. Simmerling, B. Strockbine, A.E. Roitberg, All-atom structure prediction and folding simulations of a stable protein, J. Am. Chem. Soc. 124 (38) (2002) 11258–11259.
[21] C. Obiol-Pardo, G. Alcarraz-Vizan, S. Diaz-Moralli, M. Cascante, J. Rubio-Martinez, Design of an interface peptide as new inhibitor of human glucose-6-phosphate dehydrogenase, J. Mol. Graphics Modell. 49 (2014) 110–117.
[22] J.-P. Ryckaert, G. Ciccotti, H.J.C. Berendsen, Numerical integration of the cartesian equations of motion of a system with constraints: molecular dynamics of n-alkanes, J. Comput. Phys. 23 (1977) 327–341.
[23] S.C. Lovell, I.W. Davis III, W.B. Arendall, P.I. de Bakker, J.M. Word, M.G. Prisant, D.C. Richardson, Structure validation by C-α geometry: φ, ψ and Cβ deviation, PROTEINS: Struct. Funct. Genet. 50 (2003) 437–450.
[24] R. Luthy, J.U. Bowie, D. Eisenberg, Assesment of protein models with three-dimensional profiles, Nature 356 (5) (1992) 83–85.
[25] R.A. Laskowski, M.W. MacArthur, D.S. Moss, J.M. Thornton, PROCHECK: a program to check the stereochemical quality of protein structures, J. Appl. Crystallogr. 26 (1993) 283–291.
[26] W. Humphrey, A. Dalke, K. Schulten, VMD: visual molecular dynamics, J. Mol. Graph. 14 (1) (1996) 33–38.
[27] Accelrys Software Inc, Discovery Studio Modeling Environment Release 4.0, Accelrys Software Inc., San Diego, USA, 2013.
[28] A.C. Wallace, R.A. Laskowski, J.M. Thornton, LIGPLOT: a program to gengerate schematic diagrams of protein-ligand interactions, Protein Eng. Des. Select. 8 (2) (1995) 127–134.
[29] Y.-L. Zhu, P. Beroza, D.R. Artis, Including explicit water molecules as part of the protein structure in MM/PBSA calculations, J. Chem. Inf. Modell. 54 (2013) 462–469.
[30] R. Kumari, R. Kumar, O.S.D.D. Consortium, A. Lynn, g_mmpbsa—a GROMACS tool for high-througput MM-PBSA calculations, J. Chem. Inf. Model. 54 (2014) 1951–1962.
[31] N. Homeyer, H. Gohlke, Free energy calculations by the molecular mechanics Poisson-Boltzmann surface area method, Mol. Inf. 31 (2) (2012) 114–122.
[32] W.-T. Chu, Q.-C. Zheng, Y.-J. Wu, J.-L. Zhang, C.-Y. Liang, L. Chern, H.-X. Zhang, Molecular dynamics (MD) simulations and binding free energy calculation studies between inhibitors and type II dehydroquinase (DHQ2), Mol. Simul. 39 (2) (2015) 137–144.
[33] O. Dagliyan, E.A. Proctor, K.M. D'Auria, F. Ding, N.V. Dokholyan, Structural & dynamic determinants of protein-peptide recognition, Structure 19 (12) (2011) 1837–1845.
[34] K.I.P.J. Hidari, T. Abe, T. Suzuki, Crabohydrate-related inhibitors of dengue virus entry, Viruses 5 (2013) 605–618.
[35] W.M.P.B. Wahala, A.M. de Silva, The human antibody response to dengue virus infection, Viruses 3 (2011) 2374–2395.
[36] L.Y. Kee, T.S. Kiat, H.A. Wahab, R. Yusof, N.A. Rahman, Nonsubstrate based inhibitors of dengue virus serine protease: a molecular docking approach to study binding interactions between protease and inhibitors, Asia Pac. J. Mol. Biol. Biotechnol. 15 (2) (2007) 53–59.
[37] L. Martinez, Automatic identification of mobile and rigid substructures in molecular dynamics simulations and fractional structural fluctuation analysis, PLoS One 10 (3) (2015).
[38] M. Rueda, V. Katritch, E. Raush, R. Abagyan, Simicon: a web tool for protein-ligand model comparison through calculation of equivalent atomic contacts, Bioinf. Adv. Access 26 (2010) 2784–2785.
[39] R. Day, B.J. Bennion, S. Ham, V. Daggett, Increasing temperature accelerates protein unfolding without changing the pathway of unfolding, J. Mol. Biol. 322 (2002) 189–203.

[40] T. Hou, J. Wang, Y. Li, W. Wang, Assesing the performance of the MM/PBSA and MM/GBSA methods. 1. The accuracy of binding free energy calculations based on molecular dynamics simulations, J. Chem. Inf. Model. 51 (1) (2011) 69–82.
[41] V.S. Lee, P. Tue-nguen, S. Nangola, K. Kitidee, J. Jitonnom, P. Nimmanpipug, C. Tayapiwatana, Pairwise decomposition of residue interaction energies of single chain Fv with HIV-1 P17 epitope varients, Mol. Immunol. 47 (5) (2010) 982–990.
[42] B. Kuhn, P. Gerber, T. Schulz-Gasch, M. Stahl, Validation and use of the MM-PBSA approach for drug discovery, J. Med. Chem. 48 (12) (2005) 4040–4048.
[43] L. Delgado-Soler, J. Arinez-Soriano, J.M. Granadino-Roldan, J. Rubio-Martinez, Predicting binding energies of CDK6 inhibitors in the hit-to-lead process, Theor. Chem. Acc. 128 (2011) 807–823.
[44] A. Ebadi, N. Razzaghi-Asl, M. Khoshneviszadeh, R. Miri, Comparative amino acid decomposition analysis of potent type 1 p38a inhibitors, J. Pharm. Sci. 21 (41) (2013).
[45] C.O. Pardo, Disrupting the Protein–Protein Recognition in Cancer Pathways by Molecular Docking. (PhD), Universitat de Barcelona, 2008.
[46] K. Wichapong, A. Nueangaudom, S. Pianwanit, F. Tanaka, S. Kokpol, Molecular dynamics simulation, binding free energy calculation and molecular docking of human D-amino acid oxidase (DAAO) with its inhibitors, Mol. Simul. 40 (14) (2014) 1–23.
[47] S.J. Davis, E.A. Davies, M.G. Tucknott, E.Y. Jones, P.A.V.D. Merwe, The role of charged residues mediating low affinity protein–protein recognition at the cell surface by CD2, Proc. Natl. Acad. Sci. U. S. A. 95 (1998) 5490–5494.
[48] K.K. Chaudhary, C.V.S.S. Prasad, Virtual scereening of compoinds to 1-deoxy-D-xylulose 5-phosphate reductoisomerase (DXR) from plasmodium falciparum, Bioinformation 10 (6) (2014).
[49] J.-Y. Liu, S.D. Mooney, Characterization of ligand type of estrogen receptor by MD simulation & MM/PBSA free energy analysis, Int. J. Biochem. Mol. Biol. 2 (2) (2011) 190–198.